PHYSICAL REVIEW B **92**, 121201(R) (2015)

Correct determination of low-temperature free-exciton diffusion profiles in GaAs

S. Bieker, T. Kiessling,* W. Ossau, and L. W. Molenkamp
Physikalisches Institut (EP3) der Universität Würzburg, 97074 Würzburg, Germany

(Received 23 June 2015; published 2 September 2015)

We report on low-temperature spatially resolved photoluminescence (SRPL) experiments to study the diffusion of free excitons in a 1.5-μm-thick layer of high-purity epitaxial GaAs. Extending previous SRPL experiments, we analyze the stationary diffusion profiles detected on the second LO-phonon replica of the free exciton. This allows us to circumvent the inherent interpretation ambiguities of the free-exciton zero-phonon line. Moreover, a spatially resolved line shape analysis of the $(FX) - 2\hbar\Omega_{\mathrm{LO}}$ replica provides direct experimental access to the pump-induced exciton temperature profile. We demonstrate that only resonant optical excitation prevents the buildup of a temperature gradient in the carrier system, which otherwise severely distorts the stationary and time-resolved free-exciton diffusion profiles.

DOI: 10.1103/PhysRevB.92.121201 PACS number(s): 78.55.Cr, 71.35.−y, 78.20.−e, 66.30.−h

Introduction. In spatially resolved photoluminescence experiments, the excitation laser beam is tightly focused to a few-micrometer spot size on the sample surface. Electrons, holes, and excitons, which are only created in this relatively small excitation volume, move freely through the crystal until they are eventually captured by impurities or annihilated by radiative or nonradiative decay. In high-purity semiconductors that exhibit low residual impurity concentrations, the characteristic length scale of photocarrier migration can significantly exceed the spatial extent of the pump spot. Spatially resolved photoluminescence (SRPL) detection schemes monitoring the spatial distribution of the luminescence intensity then provide direct experimental access to photocarrier transport processes. In distinction from traditional transport experiments, spatially resolved optical spectroscopy techniques obviate the application of electric fields and are not limited to the investigation of charged particles.

SRPL experiments are widely used to investigate the diffusion of photoexcited charge carriers and excitons in semiconductors and semiconductor nanostructures. Most commonly, above-band-gap illumination is used to excite a localized photocarrier packet. Diffusion coefficients are then derived from comparison of the resulting diffusion profiles to solutions of the photocarrier diffusion equation. This approach, however, may face ambiguity problems.

In this Rapid Communication, we report on SRPL experiments on a nearly defect-free GaAs layer to study the diffusion of free excitons. Our measurements reveal a peculiar dependence of the stationary exciton diffusion profile on the excitation wavelength. We unambiguously demonstrate that *only under resonant optical excitation*, the experimental diffusion profiles are correctly described by the commonly used formulation of the photocarrier diffusion equation, which assumes a spatially nonvarying diffusion coefficient. Because of localized heating in the carrier system, slight off-resonant excitation already results in severe distortions of the exciton diffusion profiles. We show that the same difficulty applies to time-resolved SRPL experiments that use pulsed optical excitation.

Sample and experimental setup. The investigated sample is a nominally undoped, 1.5-μm-thick epilayer of (001)-oriented molecular-beam-epitaxy-grown GaAs. The active layer is enclosed between one 250-period GaAs/Al$_{0.09}$Ga$_{0.91}$As superlattice on the bottom and one 80-period superlattice of identical composition on top to prevent optically excited excitons from diffusing out of the layer and to suppress surface recombination [1]. The low-temperature photoluminescence (PL) spectrum of the sample is displayed in Fig. 1(a). The dominance of the free-exciton recombination line (FX) along with the extremely weak bound exciton luminescence indicates a negligible defect concentration in the active layer. From a comparison with spectra reported in the literature [2,3], we estimate a residual impurity concentration of $\lesssim 1 \times 10^{12}$ cm^{-3}.

We use a standard confocal SRPL technique to detect spatially resolved PL profiles. The sample is mounted on the cold finger of an optical liquid-helium-flow cryostat. Tunable optical excitation is provided by a continuous wave (cw) Ti:sapphire laser. The laser beam is focused at normal incidence on the sample surface by an infinity-corrected NA = 0.4 microscope objective to a $(1/e)$ intensity spot diameter of 3.6 μm. Luminescence is collected by the same objective, focused on the entrance slit of a 1 m focal length monochromator equipped with a 1200 mm^{-1} grating, and detected by a liquid-nitrogen-cooled CCD array. Spatial information on the local PL intensity is contained in the vertical pixel number of the two-dimensional CCD image. The spatial resolution of the detector assembly is 1.0 μm.

Results and discussion. The inhomogeneous partial differential equation describing photocarrier diffusion in bulk semiconductors reads [5]

$$\frac{\partial}{\partial t} n(\mathbf{x},t) = \nabla \cdot [D \nabla n(\mathbf{x},t)] - \frac{n(\mathbf{x},t)}{\tau} + g(\mathbf{x},t), \qquad (1)$$

where $n(\mathbf{x},t)$ is the photocarrier density, D is the diffusion coefficient, τ is the photocarrier ensemble lifetime, and $g(\mathbf{x},t)$ represents the source term due to the laser excitation spot. To simplify Eq. (1), it is typically assumed that the diffusion coefficient D does not depend on the spatial coordinate $\mathbf{x}$ and that the diffusion process is isotropic. The density profile $n(\mathbf{x},t) \rightarrow n(r,t)$ then depends only on the radial distance r with respect to the pump spot and the photocarrier diffusion

---

*tobias.kiessling@physik.uni-wuerzburg.de

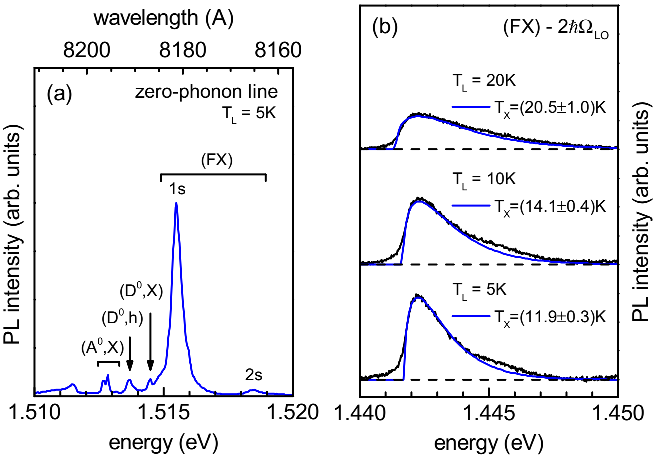

FIG. 1. (Color online) (a) Low-temperature PL spectrum of the investigated sample ($\lambda_{\text{exc}} = 8100$ Å). Text labels indicate the excitonic transitions in the usual nomenclature [4]. The spectrum is dominated by free-exciton luminescence, indicating an exceptionally low residual impurity concentration in the active layer. (b) Representative spectra of the free-exciton second LO-phonon replica $(FX) - 2\hbar\Omega_{\text{LO}}$. The spectra are vertically offset for clarity. Solid blue lines are Maxwellian fits to the data, from which we obtain the exciton temperature T_X. The gradual broadening of the asymmetrical line shape illustrates the increasing occupation of high-energy states in the tail of the Boltzmann distribution function at elevated temperatures.

equation is written in spherical coordinates as

$$\frac{\partial}{\partial t} n(r,t) = D\nabla_r^2 n(r,t) - \frac{n(r,t)}{\tau} + g(r,t). \tag{2}$$

Analytical solutions to Eq. (2) are not found for some widely used sample geometries, e.g., a three-dimensional half-space. The experiments presented in this study are, therefore, performed on a 1.5-μm thin GaAs epilayer. The diffusion length here exceeds the thickness of the active layer by approximately one order of magnitude (see discussion below), rendering the lateral diffusion of free excitons in our sample effectively a two-dimensional problem [6].

The Green's function solution to the two-dimensional stationary photocarrier diffusion equation for a continuous wave point source $g(r) = \delta(r)$ is given by [7,8]

$$G(r) = \frac{1}{2\pi D} K_0\left(\frac{r}{\sqrt{D\tau}}\right), \tag{3}$$

where K_0 denotes the zeroth-order modified Bessel function of the second kind. The characteristic length scale $L = \sqrt{D\tau}$ is commonly referred to as the *diffusion length*. The stationary diffusion profile $n(r)$ for an arbitrary source term $g(r)$ (e.g., a Gaussian laser spot) is then obtained from a convolution of the Green's function solution $G(r)$ with the excitation profile $g(r)$.

To compare experimental free-exciton diffusion profiles with the density profiles expected from Eq. (3), we first consider the appropriate detection wavelength. During the free-exciton luminescence process, the entire exciton energy and momentum must be imparted to the emitted photon. Because of the relatively small photon wave vectors k_ν, only a subset of the entire free-exciton ensemble close to the Brillouin zone center with $K = k_\nu \approx 0$ contributes to the (FX) zero-phonon line [9–11]. In particular, hot excitons that exhibit relatively large K vectors are protected against radiative decay. Consequently, the spatially resolved emission intensity of the (FX) transition is not a direct measure of the actual free-exciton density in the crystal. The interpretation of diffusion profiles detected on the (FX) zero-phonon line is, therefore, inherently ambiguous.

A competing process to the direct annihilation of free excitons is the radiative decay under simultaneous emission of two LO phonons. In contrast to the zero-phonon line, excitons with considerably larger wave vectors can decay radiatively via the free-exciton second LO-phonon replica $(FX) - 2\hbar\Omega_{\text{LO}}$. This is because the wave vectors of the two LO phonons can always add up such that they compensate for the center-of-mass momentum of the recombining exciton.

Representative $(FX) - 2\hbar\Omega_{\text{LO}}$ spectra are shown in Fig. 1(b). The replica is redshifted with respect to the zero-phonon line by two times the GaAs LO-phonon energy $\hbar\Omega_{\text{LO}} = 36.8$ meV [12]. Because of the fully relaxed K vector selection rule, the recombination line shape of the second LO-phonon replica mirrors the density of occupied states of the thermalized free-exciton ensemble. We can, therefore, obtain the exciton temperature T_X from a Maxwellian line shape analysis of the $(FX) - 2\hbar\Omega_{\text{LO}}$ transition [13,14]. Moreover, the spectrally integrated emission intensity of the two-LO-phonon sideband is directly proportional to the actual free-exciton density [15].

To avoid the inherent interpretation ambiguities of the previously investigated zero-phonon line and to monitor the *total* free-exciton density, we assess the exciton diffusion profiles by the spectrally integrated emission intensity of the extremely weak $(FX) - 2\hbar\Omega_{\text{LO}}$ replica.

We show in Fig. 2 the transformation of the free-exciton diffusion profile as a function of the excitation wavelength λ_{exc}. Under resonant optical excitation at the free-exciton resonance [$\lambda_{\text{exc}} = 8180$ Å; cf. Fig. 1(a)], the diffusion profile reveals the characteristic Bessel function shape associated with the analytical solution of the stationary photocarrier diffusion equation in two spatial dimensions [Eq. (3)]. From a fit to the data (solid red line) we obtain the diffusion length $L = (10.5 \pm 0.3)$ μm. The large diffusion length L, which significantly exceeds the 1.5 μm thickness of the active GaAs layer, renders our sample effectively two-dimensional [6] and justifies *a posteriori* our expectation that the diffusion process is described by the two-dimensional (2D) photocarrier diffusion equation. Assuming a free-exciton lifetime $\tau = 3$ ns [11], the observed diffusion length corresponds to an exciton diffusion coefficient of $D = (371 \pm 24)$ cm^2 s^{-1}.

As we tune λ_{exc} to shorter wavelengths (i.e., larger excess energies), the characteristic cusp around the excitation center is washed out and the diffusion profile flattens. A significant rounding of the profile is already seen at $\lambda_{\text{exc}} = 8150$ Å, which corresponds to an electron excess energy of merely 2 meV [16]. For comparison and to highlight the deviation from the analytical 2D solution, we show the fit to the data set obtained under resonant optical excitation by the dash-dotted line.

When the excitation excess energy is further increased, the flattening of the diffusion profile progressively evolves into

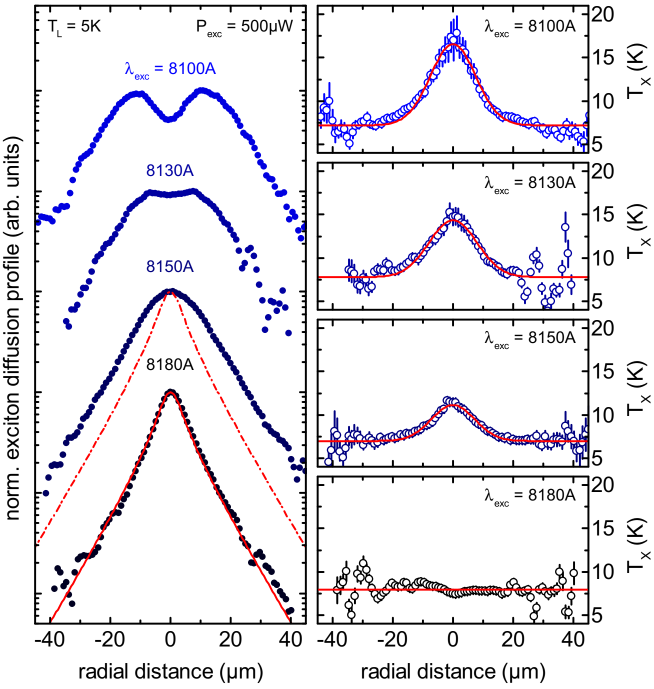

FIG. 2. (Color online) Transformation of the stationary free-exciton diffusion profile as a function of the excitation wavelength. The profiles are vertically offset for clarity. Data points indicate the spectrally integrated emission intensity of the $(FX) - 2\hbar\Omega_{\rm LO}$ replica, the spectral line shape of which provides direct access to the corresponding exciton temperature profile $T_X(r)$. The resulting diffusion profile is correctly described by the stationary solution of the two-dimensional diffusion equation (solid red line) only for resonant optical excitation ($\lambda_{\rm exc} = 8180$ Å). Slight off-resonant optical excitation ($\lambda_{\rm exc} = 8150$ Å) causes already a localized overheating of the exciton ensemble, which results in severe distortions of the experimental exciton density profile.

a pronounced quench of the free-exciton density around the excitation spot.

To elucidate the reason for this peculiar transformation of the stationary diffusion profile, we plot in Fig. 2 the corresponding exciton temperature profiles $T_X(r)$ obtained from spatially resolved Maxwellian line shape analyses of the $(FX) - 2\hbar\Omega_{\rm LO}$ replica [13,14]. Only in the case of resonant optical excitation at $\lambda_{\rm exc} = 8180$ Å, the exciton temperature profile is flat, i.e., T_X is constant at all distances from the pump spot. A deviation of the exciton temperature $T_X \approx 8$ K from the lattice temperature $T_L = 5$ K has been observed in previous SRPL experiments [17,18] and is a consequence of the recombination heating effect [19,20]. More importantly, Fig. 2 demonstrates that only slightly off-resonant optical excitation ($\lambda_{\rm exc} = 8150$ Å) suffices to cause a local hot spot in the exciton system, whose peak temperature $T_X(r = 0)$ increases with increasing excess energies.

The distortion of the experimental diffusion profile is unambiguously correlated with the localized overheating of the exciton cloud, which affects the exciton diffusion profile in two distinct ways.

(i) The stationary solution to the photocarrier diffusion equation was derived under the assumption of a spatially nonvarying diffusion coefficient D. This seemingly natural approximation fails under the practical excitation conditions in most spatially resolved spectroscopy experiments. Such experiments necessitate the use of focused laser sources, which unavoidably cause a local overheating at the pump spot. Since the diffusion coefficient is typically a strong function of the temperature [21–24], local heating directly renders the diffusion coefficient $D \rightarrow D[T_X(r)]$ spatially dependent. Such heating effects have previously been shown to influence the steady-state electron spin diffusion profiles in GaAs [25] and also prominently alter the transient diffusive expansion of an electron spin packet following pulsed optical excitation [26].

(ii) The exciton temperature also crucially influences the thermodynamic population balance between free excitons and unbound charge carriers described by the Saha equation [27,28]. An overheating of the photocarrier ensemble at the pump spot causes the thermal breakup of Coulomb-bound excitons into uncorrelated electron-hole pairs that eventually manifest as a macroscopic free-exciton luminescence ring around the excitation spot [18].

The heavy distortions of experimental diffusion profiles due to pump-induced temperature gradients in the carrier system are not limited to cw SRPL spectroscopy. Another widely employed technique for the study of charge carrier and exciton diffusion is photoluminescence spectroscopy with simultaneous time and spatial resolution. Diffusion coefficients are then obtained from the diffusive expansion rate of a Gaussian

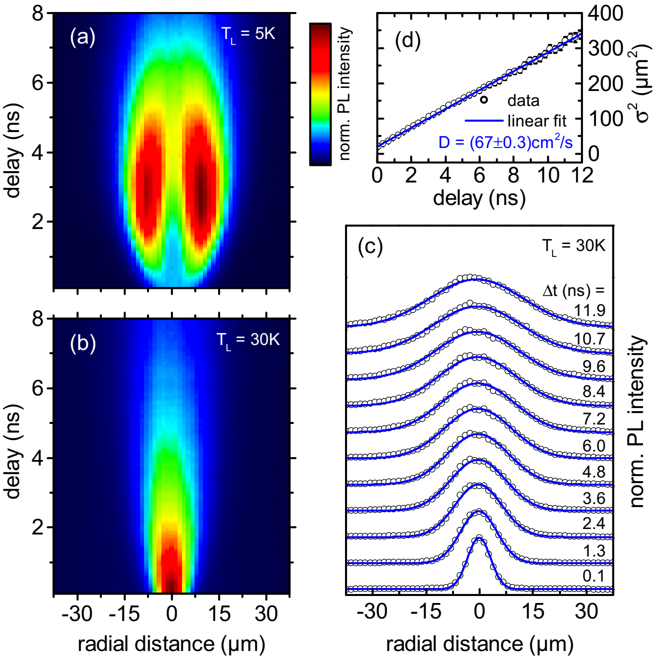

FIG. 3. (Color online) (a) Time and spatially resolved free-exciton photoluminescence response to a focused picosecond excitation pulse ($\lambda_{\rm exc} = 7500$ Å, $P_{\rm exc} = 3$ μW). Color indicates the emission intensity of the (FX) zero-phonon line. At short delays, the exciton density exhibits a localized quench at the excitation center due to a pump-induced hot spot. (b) This ring formation disappears at $T_L \gtrsim 30$ K. (c) The spatial diffusion profile of the exciton cloud then remains Gaussian for all times. (d) The corresponding diffusion coefficient is obtained from a linear fit to the time-dependent squared width of the instantaneous diffusion profiles.

photocarrier packet [29]. The momentary diffusion profiles are, however, equally affected by a pump-induced hot spot.

To demonstrate this effect, we show in Fig. 3 the spatiotemporal expansion of a free-exciton cloud following nonresonant pulsed excitation [30]. We here trace the time-resolved diffusion profiles by the emission intensity of the (FX) zero-phonon line since the inherent intensity weakness of the second LO-phonon replica renders time-resolved SRPL spectroscopy of the $(FX) - 2\hbar\Omega_{\mathrm{LO}}$ transition unfeasible. Naturally, detection at the (FX) resonance is a major obstacle for resonant optical excitation at the same wavelength.

We first consider low sample temperatures [$T_L = 5$ K; Fig. 3(a)]. At short time delays Δt with respect to the laser pulse, the exciton density exhibits a pronounced quench around the pump spot. This ring formation is the same as seen in Fig. 2 under cw optical excitation. Clearly, the experimental diffusion profiles cannot be fitted with straightforward Gaussians, impeding a robust determination of the diffusion coefficient.

Only in the absence of temperature gradients in the carrier system does an initially Gaussian photocarrier packet remain Gaussian at all times. This is demonstrated in Figs. 3(b) and 3(c) where we show the same measurement performed at 30 K lattice temperature. At such elevated sample temperatures, the availability of LO-phonon emission as an efficient channel for excess energy relaxation prevents the buildup of temperature gradients in the carrier system [18,31]. Only then is the diffusive expansion of the photocarrier cloud correctly described by the time-dependent solution of the diffusion equation (2). The diffusion coefficient D is then readily obtained from the linear increase of the squared $(1/e)$ width $\sigma^2(\Delta t) = \sigma_0^2 + 4D\Delta t$ of the Gaussian photocarrier packet [29]. In our high-purity GaAs layer, we find a photocarrier diffusivity of $D = (67.0 \pm 0.3)\ \mathrm{cm}^2\,\mathrm{s}^{-1}$ at $T_L = 30$ K [Fig. 3(d)] [32].

Summary and conclusion. We have investigated the diffusion of free excitons in a piece of nearly defect-free GaAs using the SRPL technique. Our analysis yields the important result that undistorted stationary and time-resolved exciton diffusion profiles, which are correctly described by the commonly used formulation of the photocarrier diffusion equation, are only observed in the absence of temperature gradients in the carrier system. At low sample temperatures, this requires strictly resonant optical excitation.

Because of the high excitation densities at the pump spot, off-resonant optical excitation results in a local hot spot that causes severe distortions of the free-exciton diffusion profiles. Such a local overheating at the pump spot is inherent to virtually all spatially resolved spectroscopy techniques involving focused laser excitation and low sample temperatures. Strictly resonant optical excitation is thus crucial for the reliable determination of diffusion coefficients from SRPL spectroscopy, a fact which has not been considered in most previous studies reported in the literature.

Acknowledgments. The excellent GaAs sample was grown at Philips Research Laboratories, Redhill, UK by J. J. Harris and C. T. Foxon. Financial support by the DFG (SPP1285 OS98/9-3) is gratefully acknowledged.

---

[1] R. J. Nelson and R. G. Sobers, J. Appl. Phys. **49**, 6103 (1978).

[2] U. Heim and P. Hiesinger, Phys. Status Solidi B **66**, 461 (1974).

[3] J. Aaviksoo, I. Reimand, V. V. Rossin, and V. V. Travnikov, Phys. Rev. B **45**, 1473 (1992).

[4] M. R. Brozel and G. E. Stillman, *Properties of Gallium Arsenide* (INSPEC, London, 1996).

[5] J. Crank, *The Mathematics of Diffusion* (Clarendon Press, Oxford, 1979).

[6] D. J. Wolford, G. D. Gilliland, T. F. Kuech, J. A. Bradley, and H. P. Hjalmarson, Phys. Rev. B **47**, 15601 (1993).

[7] T. Myint-U and L. Debnath, *Linear Partial Differential Equations for Scientists and Engineers* (Birkhäuser, Boston, 2007).

[8] M. Furis, D. L. Smith, S. Kos, E. S. Garlid, K. S. M. Reddy, C. J. Palmstrøm, P. A. Crowell, and S. A. Crooker, New J. Phys. **9**, 347 (2007).

[9] E. F. Gross, S. A. Permogorov, and B. S. Razbirin, Phys. Usp. **14**, 104 (1971).

[10] J. Feldmann, G. Peter, E. O. Göbel, P. Dawson, K. Moore, C. Foxon, and R. J. Elliott, Phys. Rev. Lett. **59**, 2337 (1987).

[11] G. W. 't Hooft, W. A. J. A. van der Poel, L. W. Molenkamp, and C. T. Foxon, Phys. Rev. B **35**, 8281(R) (1987).

[12] J. S. Blakemore, J. Appl. Phys. **53**, R123 (1982).

[13] E. Gross, S. Permogorov, and B. Razbirin, J. Phys. Chem. Solids **27**, 1647 (1966).

[14] B. Segall and G. D. Mahan, Phys. Rev. **171**, 935 (1968).

[15] In principle, T_X can also be obtained from a line shape analysis of the first LO-phonon replica of the free-exciton transition [13,33]. Although the one-LO phonon assisted recombination line offers the advantage of being more intense than the second LO-phonon replica, the severe distortion by the spectrally nearby (e,A^0) and (D^0,A^0) transitions renders a robust line shape analysis of the first LO-phonon replica unfeasible.

[16] C. Weisbuch, Solid-State Electron. **21**, 179 (1978).

[17] S. Bieker, T. Henn, T. Kiessling, W. Ossau, and L. W. Molenkamp, Phys. Rev. B **90**, 201305(R) (2014).

[18] S. Bieker, T. Henn, T. Kiessling, W. Ossau, and L. W. Molenkamp, Phys. Rev. Lett. **114**, 227402 (2015).

[19] D. Bimberg and J. Mycielski, Phys. Rev. B **31**, 5490 (1985).

[20] A. L. Ivanov, J. Phys.: Condens. Matter **16**, S3629 (2004).

[21] C. M. Wolfe, J. Appl. Phys. **41**, 3088 (1970).

[22] J. P. Wolfe, J. Lumin. **53**, 327 (1992).

[23] J. Erland, B. S. Razbirin, K. H. Pantke, V. G. Lyssenko, and J. M. Hvam, Phys. Rev. B **47**, 3582 (1993).

[24] B. A. Ruzicka, L. K. Werake, H. Samassekou, and H. Zhao, Appl. Phys. Lett. **97**, 262119 (2010).

[25] J. H. Quast, T. Henn, T. Kiessling, W. Ossau, L. W. Molenkamp, D. Reuter, and A. D. Wieck, Phys. Rev. B **87**, 205203 (2013).

[26] T. Henn, T. Kiessling, W. Ossau, L. W. Molenkamp, D. Reuter, and A. D. Wieck, Phys. Rev. B **88**, 195202 (2013).

[27] W. D. Kraeft, K. Kilimann, and D. Kremp, Phys. Status Solidi B **72**, 461 (1975).

[28] G. Bastard, *Wave Mechanics Applied to Semiconductor Heterostructures* (Halsted, New York, 1988).

[29] H. W. Yoon, D. R. Wake, J. P. Wolfe, and H. Morkoç, Phys. Rev. B **46**, 13461 (1992).

[30] Slightly different excitation and PL detection schemes are used to acquire time and spatially resolved diffusion profiles. Above-band-gap optical excitation at $\lambda_{\mathrm{exc}} = (750 \pm 40)$ nm is provided by the spectrally sliced output of a picosecond supercontinuum fiber-laser source [34]. The monochromator entrance slit assembly is replaced by a 50-μm-diameter pinhole to select luminescence from a well-defined position on the sample surface. Time-resolved PL signals of the (FX) transition are detected by the standard time-correlated single photon counting technique [35].

[31] R. Ulbrich, Phys. Rev. B **8**, 5719 (1973).

[32] We note that the diffusion coefficient at $T_L = 30$ K is not a pure exciton diffusion coefficient, but that of the partially ionized exciton gas, which involves a significant fraction of unbound electron-hole pairs [27,18].

[33] D. Kovalev, B. Averboukh, D. Volm, B. K. Meyer, H. Amano, and I. Akasaki, Phys. Rev. B **54**, 2518 (1996).

[34] T. Henn, T. Kiessling, W. Ossau, L. W. Molenkamp, K. Biermann, and P. V. Santos, Rev. Sci. Instrum. **84**, 123903 (2013).

[35] W. Becker, *Advanced Time-Correlated Single Photon Counting Techniques* (Springer, Berlin, 2005).